

Tensile Behavior Simulation of Woven Fabric with Different Weave Pattern Based on Finite Element Method

Majid Tehrani-Dehkordi and Hooshang Nosraty

Abstract—The properties and structure of the yarns within the fabric generate a complex mechanism of deformation. Although many literatures are available on mechanical properties of woven fabrics, little micro-mechanical information have become public on tensile behavior of such materials. In this study, the tensile behavior of woven fabrics with different weave patterns is simulated by using finite element method. Yarn geometry parameters are measured with the help of microscopy and image processing techniques. Three-dimensional geometrical models are simulated by use of fabric geometry data. To evaluate the proposed model, the numerical results are compared to the experimental measurements. The results show that by using the three dimensional modeling of fabric and precisely imparting the yarn properties in the finite element program, the tensile properties of fabric with different weave patterns can be reasonably predicted.

Keywords: Simulation, finite element method, tensile behavior, woven fabric, weave pattern

I. INTRODUCTION

Mechanical properties of woven fabrics can be characterized in terms of yarn properties and fabric structures. Many studies have been made on the determination of mechanical properties of woven fabrics [1]. Attempts of modeling of woven structures trace back to the beginning of the twentieth century. The main goal of the mechanical modeling consists in a description of the nature of the efforts exerted within the pattern and their distribution on the contact area between two threads. The reported mechanical models within the literature can be classified into three different categories, i.e. the geometrical models give an essentially geometrical description of the structure [2-7], the mechanical models deal with the description of the efforts exerted on a fabric sample and their relationship to the fabric deformation [8-10], while energetic models handle the constitutive behavior of the fabric as an energy minimization problem [11-13].

The geometrical studies of Peirce [2] provided the basis for the first approach, which its modifications were subsequently introduced [3-5]. Peirce's paper [2] contains a mechanical model for determining the shape of elastic yarns in a plain weave fabric subject to equal and opposite lateral pressures at their contact point. Olofsson [6]

extended the mechanical approach to include external tensions and bending moments. More recently, de Jong and Postle [14-15] developed a model of fabric structure based on energy relations rather than force equations [7, 16].

In the early stages of computers age, finite element (FE) were rapidly implemented to simulate the mechanical behavior of plain weave structure, providing a more accurate insight on this subject. FE method provides the detailed shape assumed by the yarn axis for each of the yarn systems in the fabric such as crimp height, crimp angle, and yarn-spacing [17, 18]. The ability of the FE method to predict the detailed shape of the yarn axes as well as the yarn diameters provide the possibility to include the geometrical aspects of jamming within the analysis and investigate the condition when the interlaced yarns are in contact over a continuous region rather than simply at a point. Several researchers investigated the mechanical behavior of woven fabrics using FE method. Among the publications in this area, Shen *et al.* [19] simulated the tensile behavior of plain weave woven fabrics using finite element method. Hou and his coworkers [20] investigated the numerical simulation of the impact tension behaviors of 3-D orthogonal woven fabric under high strain rates and compared the results to those obtained under quasi-static tension. Wang *et al.* [21] analyzed the tongue-tearing behaviors of plain and twill woven fabric based on the microstructure model. Jeong and Kang [22] proposed a computer model for analyzing the compression deformation behavior of a woven fabric in the three-dimensional viewpoint. To improve the comprehension of woven fabric behavior, Dridi *et al.* [23] developed an orthotropic hyper-elastic continuum model of woven fabric. The model covered the influence of the ratio between shearing and tensile rigidities of woven fabric on stress and strain fields. Lin [24] employed a geometrical modeling based on slice array model to predict the elastic property (i.e. initial Young's modulus) of plain weave woven fabric. Zouari *et al.* [25] employed the numerical tensile analysis in seven directions of plain weave woven fabric to ensure their homogeneity. In order to better understand the drape phenomenon of fabrics, Kang and Yu [26], Hedfi and his coworkers [27] and Mingxiang *et al.* [28] simulated the macro-mechanical three-dimensional drape shapes of a woven fabric by using the non-linear FE code. Khadamalhosseini and his colleagues [17] developed a computational model to simulate the effect of sewing

M. Tehrani Dehkordi is with the Department of Carpet, Shahrekord University, Shahrekord, Iran. H. Nosraty is with the Department of Textile Engineering, Tehran, Iran. Correspondence should be addressed to M. Tehrani Dehkordi (e-mail: mtehrani@lit.sku.ac.ir).

TABLE I
RESULTS OF KEMP'S MODEL PARAMETERS FOR DIFFERENT FABRIC WEAVE PATTERN

Fabric pattern	Test direction	Fabric density (cm ⁻¹)	Crimp of yarn (%)	a (mm)	b (mm)	p (mm)	l (mm)	l' (mm)	θ (degree)	h (mm)
Plain	Warp	20.0	14.5	0.36	0.18	0.50	0.65	0.45	51	0.24
	Weft	17.5	4.0	0.34	0.20	0.57	0.52	0.36	57	0.16
Twill	Warp	21.0	11.2	0.34	0.18	0.48	0.69	0.53	72	0.28
	Weft	17.5	5.0	0.36	0.20	0.57	0.52	0.36	49	0.15
Satin	Warp	21.0	4.5	0.34	0.20	0.46	0.69	0.55	59	0.30
	Weft	17.5	5.5	0.36	0.24	0.59	0.54	0.42	65	0.18

machine needle impact on woven fabrics.

Although many literatures such as the aforementioned models are available on the mechanical properties of plain weaved woven fabrics, a very few reports on micro-mechanical information are available about the tensile behavior of other weave patterns. In this study, the tensile behavior of some weave patterns (plain, twill, satin) was simulated in three-dimensional viewpoint using FE method. The validity of model was examined by the results of experiments obtained from cotton woven fabrics.

II. NUMERICAL MODEL

A. Fabric structure parameters

Woven fabrics were produced by interlacing two orthogonal sets of yarns, warp and weft. Depending on the type of interlacement, a variety of weaves patterns including plain, twill and satin would be produced.

The cross-sectional shapes and the centerline configurations of the constituent yarns mainly determine the fabric geometric structures. The cross-sectional shapes of the yarns within the fabrics may be circular, ellipsoidal, or racetrack. In fact, based on the weave patterns, the tightness of construction, the finishing treatment and the cloth construction they could be varied quickly.

Peirce [2] first presented a rather intensive analysis of woven fabric structure by considering the geometric form of the yarn configuration. In this model, he assumed that the cross-sectional shapes of woven threads are circular. With normal kinds of woven fabrics, it can find that the assumption of a circular thread cross-section is invalid. To overcome this difficulty, Kemp [5] modified the shape of yarn cross-section within a fabric. As Fig. 1 shows, he adopted the shape called racetrack section which encloses a rectangle between semicircular ends.

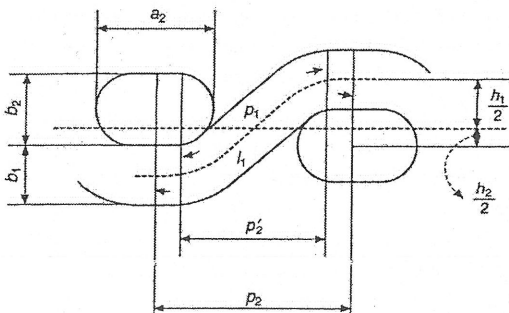


Fig. 1. Configuration of yarns in Kemp's model [5].

In this study, the Kemp's model was used to simulate the structure of plain, twill 3/1 and satin 8 fabrics using Abacus software. Details of yarns and fabrics parameters for different weave patterns are summarized in Table I. In this table, the crimp of yarns was obtained from the extension in yarns that was measured by an Instron tensile tester. Diameter of yarns were measured with provide of fabric cross-sections and using microscopy images. The fabric density was obtained with the standard counting lens.

To obtain the fabric geometry, the Kemp equations [5] were solved by using yarn crimp, yarn diameters and fabric density. The employed equations are:

$$l'_i = l_i - a_i + b_i \quad (1)$$

$$D = b_i + b_j \quad (2)$$

$$p_i = a_i - b_i + (l'_j - D\theta_j + D\sin\theta_j) \quad (3)$$

$$h_i = (l'_i - D\theta_i)\sin\theta_i + D(1 - \cos\theta_i) \quad (4)$$

where, θ and l' are the angle and half-length of yarn in undulation section of each wave repetition. The subscripts of i and j are used to denote the warp and weft direction, respectively. Other symbols are shown in Fig. 1. The results of Kemp's equations are given in Table I.

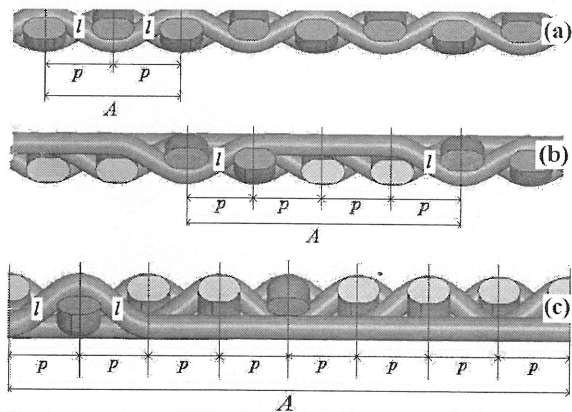


Fig. 2. Interlacing of warp and weft yarns in fabrics with (a) plain, (b) twill 3/1 and (c) satin 8 weave patterns.

To estimate l in Equation 1, the yarns were assumed straight except in undulation sections. Figure 2 shows the interlacing of warp and weft yarns in fabrics with different weave pattern. In this figure, "A" denotes the wave repetition. According to this figure, Equations 5 to 7 can be used for calculating the value of l in plain, twill 3/1 and satin 8 fabrics, respectively.

$$l = \frac{B}{2} \quad (5)$$

$$l = \frac{B - 2P}{2} \quad (6)$$

$$l = \frac{B - 6P}{2} \quad (7)$$

In these equations, “B” is the length of yarn in each wave repetition (“A”).

B. Assumptions

The following assumptions for numerical modeling were considered:

- The geometry of yarns surface was assumed to be smooth and uniform (which was not smooth really due to the fine hairs on the yarn surface). Therefore, the resistance of the fine hairs on the yarns surface was ignored.

- The fabrics were assumed to be completely relaxed. It means that the fabrics did not have any residual stress within itself.

- The longitudinal geometry of yarns was assumed monotonic without any thin and/or thick places.

C. Finite element model

The tensile properties of woven fabrics with different weave patterns were simulated based on FE method. For simulation, some stages such as part, assembly, property, contact properties, boundary condition, mesh and solve were performed in the Abaqus software version 6.4 with following specifications [29].

In the part stage, the yarns were simulated solid, homogenous isotropic and deformable, as shown in Fig. 3. After that, woven fabric with different weave patterns were created by interlacing the simulated yarns in assembly stage.

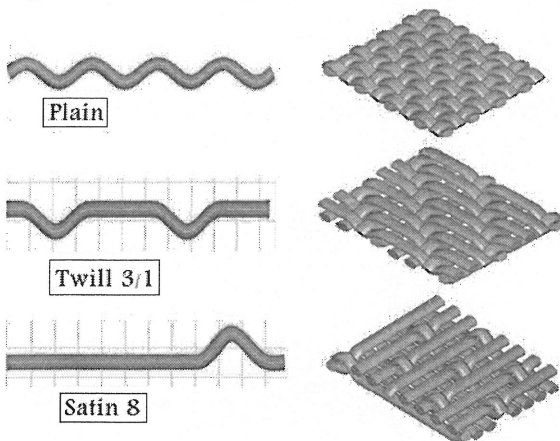


Fig. 3. Models of yarns and fabrics in abaqus software.

The physical and mechanical parameters of yarns such as tensile behavior, Poisson’s ratio and density were determined in Abaqus software. These parameters were characterized from Instron tensile tester and reference [30]. Tensile behavior of yarns was determined in the elastic-plastic phase. The elastic phase (before yield point) was determined with elastic modulus. The plastic phase (yield point up to rupture point) was determined by some points

of plastic region at load-elongation curves. Figure 4 shows the definition of elastic-plastic behavior of yarns in Abaqus software. The physical and mechanical properties of simulated yarns are summarized in Table II. The properties were obtained from extracted yarns of woven fabrics, experimentally. “Maximum principle stress” (Maxps damage) criterion was used as strength criterion. In this strength criterion, longitudinal stress of each element in principal material coordinates must be less than the respective strength; otherwise, rupture is said to have occurred on that element [29].

TABLE II
THE PHYSICAL AND MECHANICAL PROPERTIES OF YARNS

Elastic modulus (Mpa) along		Poisson ratio	Density (kg/m ³)
Warp	Weft		
2.25	1.88	0.001	1100

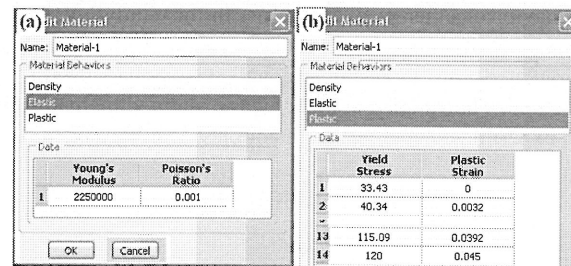


Fig. 4. Definition of (a) elastic and (b) plastic behaviors of yarns in Abaqus software.

The yarns were meshed by C3D8R element type with the size of 0.1 mm. This type of mesh had uniform, 3D solid and brick structure, which is shown in Fig. 5.

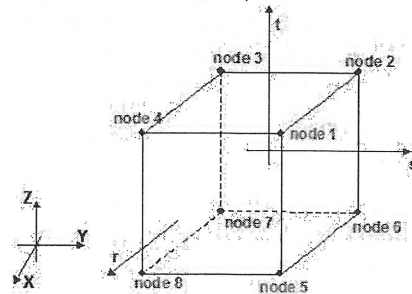


Fig. 5. Eight-node brick element.

Surface-to-surface contact-element was used to represent the contact between warp and weft yarns. The friction coefficient of 0.23 was assumed in all analyses [31].

Before describing the boundary condition, several notations were defined. u_x , u_y and u_z represent the displacements in x, y and z directions, respectively. In addition, ϕ_x , ϕ_y and ϕ_z are rotations around the x, y and z-axes. With respect to these notations, the boundary conditions were defined that could be described as follows. The boundary conditions were imposed on the two ends of the fabrics as shown in Fig. 6. One side fixed in all directions, while the other side was movable with constant velocity. It means that $u_x=u_y=u_z=\phi_x=\phi_y=\phi_z=0$ on a fixed side and on the other side, all degree of freedoms are fixed expect u_x and u_y .

All tensile processes were carried out at a constant cross-head speed. The velocity of tensile operation for different weave pattern along warp and weft directions is summarized in Table III. These cross-head speeds were calculated according to the dimension of the analyzed unit cell.

The explicit solver was used for final analyses in Abaqus package. Explicit finite element codes were used to solve non-linear analysis problems. This type of code could be therefore ideal for the analysis of fabric structure where material behavior can be highly non-linear and large deformations occur [32]. Three-point gauss method for equations solving was used. The results of these analyses summarized as follow. Figure 7 shows typical tensile processes for twill weave pattern along warp direction.

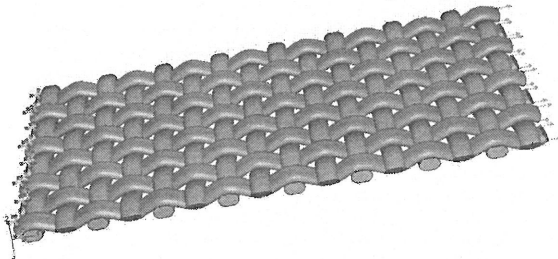


Fig. 6. The imposed boundary conditions on the two ends of fabrics.

TABLE III
THE CROSS-HEAD SPEED OF TENSILE OPERATION FOR DIFFERENT SPECIMENS

Weave pattern	Test direction	Velocity(Lm/s)
Plain	Warp	69.2
	Weft	39.8
Twill	Warp	57.1
	Weft	42.1
Satin	Warp	40.8
	Weft	44.3

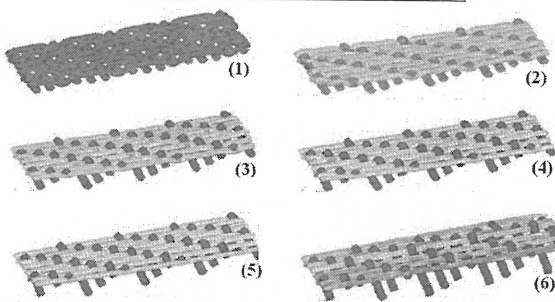


Fig 7. Tensile processes for twill weave along warp direction.

III. EXPERIMENTAL PROCEDURE

To evaluate the simulated model, three types of fabric with different woven structures were produced. The cotton yarn was used in the count of 24 Ne at the warp and weft directions.

All sample fabrics were tested by using an Instron tensile tester equipped with a 10 kN load cell along the warp and weft directions. The tests were carried out on rectangular specimens with a length of 200 mm and a width of 50 mm. The tensile tests were performed at temperature of $22 \pm 2^\circ\text{C}$ and relative humidity of $50 \pm 2\%$. All measurements were carried out at a constant cross-head speed on at least eight specimens. The experimental results obtained for various woven structures are summarized in Table IV.

TABLE IV
EXPERIMENTAL RESULTS OF VARIOUS FABRICS

Fabric pattern	Test direction	Maximum load (N)	Tensile strain (%)
Plain	Warp	774	18.6
	Weft	656	8.4
Twill	Warp	741	15.6
	Weft	574	9.2
Satin	Warp	682	10.1
	Weft	502	9.8

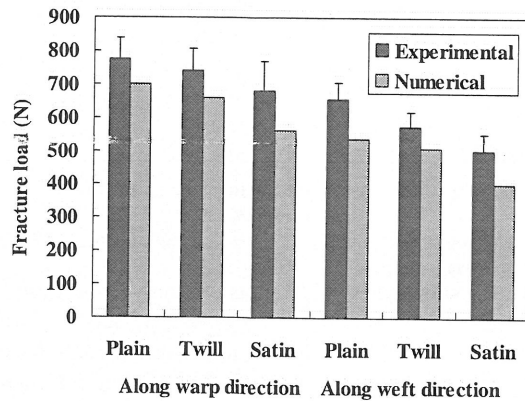


Fig. 8. Experimental and numerical rupture load for different weave patterns.

IV. RESULTS AND DISCUSSION

In order to evaluate the numerical results, the rupture load of different weave patterns (plain, twill and satin) were compared with experimental results in Table V. The obtained results in this table show that there is a reasonable correlation between the numerical and experimental results. It can be realized that the maximum difference between numerical and experimental results is about 20%. The reason of this difference is the assumptions that made in modeling section and experimental errors. To improve the numerical results and reach the real fabric model, the mentioned assumptions have to be modified or even corrected.

The experimental and numerical rupture load of different weave patterns along warp and weft directions are compared in Fig. 8. This figure shows that on both

TABLE V
NUMERICAL AND EXPERIMENTAL RESULTS OF DIFFERENT WEAVE PATTERNS

Fabric pattern	Rupture load (N) along warp direction			Rupture load (N) along weft direction		
	Experimental	Numerical	Difference (%)	Experimental	Numerical	Difference (%)
plain	774	699	9.7	656	535	18.5
Twill	741	660	10.1	574	507	11.7
Satin	682	562	17.6	502	400	20.3

directions, the plain and satin weave patterns have the highest and least rupture load, respectively. The satin weave pattern has less undulation than the plain one. Therefore, the satin weave must have more rupture load respect to the plain one. The frictions between warp and weft yarns caused to variant these results. Among the studied fabric weave patterns, the plain weave pattern has the highest friction load between warp and weft yarns therefore; the highest rupture load belongs to the fabric with plain weave pattern. For the fabric that used in this research, the friction load respect to the yarn undulation has more influence on rupture load. In Abacus package, frictions between the warp and weft yarns were performed using the surface-to-surface method.

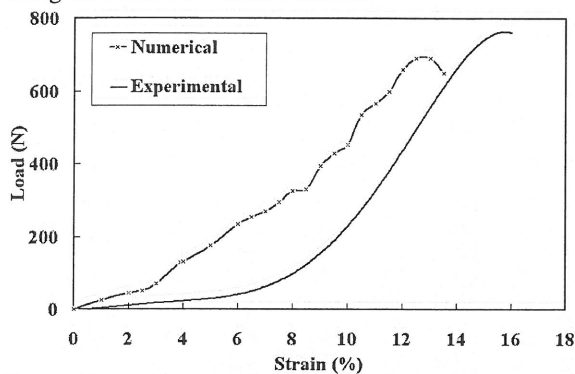


Fig. 9. Numerical and experimental curves of load vs. strain for plain weave along warp direction.

Figure 9 shows the typical plots of load versus strain for plain weave pattern along warp direction, obtained from instrumented tensile testing and numerical model. As the figure shows, the numerical curve has a good correlation with the experimental curves. The results show that the applied load in each strain can be eligible determined from numerical curve.

V. CONCLUSIONS

In this study, a numerical model based on FE method was proposed for predicting the tensile properties of fabrics with different weave patterns. From the results, the following conclusions can be obtained:

- By assuming the straight behavior for yarns (except in undulation sections), Kemp's model can be utilized as a proper model for extraction the initial information of twill and satin fabric structures.

- By using the three dimensional modeling of fabric and precisely imparting the yarn properties in the Abacus package, the tensile properties of fabric with different weave patterns can be reasonably predicted.

- A good correlation between the numerical and experimental load-strain curves is possible. Therefore, the proposed numerical model can be determined the applied load in each strain.

- The numerical and experimental results showed that the highest and least rupture loads belong to the plain and satin weave patterns, respectively.

- For applying the friction load in 3D model, surface-to-surface was found to be the best method in Abacus

package.

Acknowledgment

The work described in this paper was supported by a grant from the Research Committee of the Shahrekord University.

REFERENCES

- [1] K. Hosseini, A. Sadeghi and A. A. Asgharian Jeddi, "Characterization of fabric tensile loading curve in nonlinear region related to their structure; Part I: Woven Fabric", *J. Text. & Polym.*, vol. 1, no. 2, pp. 53-59, 2013.
- [2] F. T. Peirce, "The geometry of cloth structure", *J. Text. Inst.*, vol. 28, pp. 45-96, 1937.
- [3] G. M. Abbott, P. Grosberg and G. A. V. Leaf, "The elastic resistance to bending of plain-woven fabrics", *J. Text. Inst.*, vol. 64, pp. 346-362, 1973.
- [4] L. Love, "Graphical relationships in cloth geometry for plain, twill, and sateen weaves", *Text. Res. J.*, vol. 24, pp. 1073-1083, 1954.
- [5] A. Kemp, "An extension of peirce's cloth geometry to the treatment of non-circular threads", *J. Text. Inst.*, vol. 49, pp. 44-47, 1958.
- [6] B. Olofsson, "A general model of a fabric as a geometric-mechanical structure", *J. Text. Inst.*, vol. 55, pp. 541-557, 1964.
- [7] S. De Jong and R. Postle, "An energy analysis of woven fabric mechanics by means of optimal control theory, Part I: Tensile properties", *J. Text. Inst.*, vol. 68, pp. 307-361, 1977.
- [8] J. Hofstee and F. Van Keulen, "3-D geometric modeling of a draped woven fabric", *Compos. Struct.*, vol. 54, pp. 179-195, 2001.
- [9] R. N. Hing and R. L. Grimsdale, "Computer graphics techniques for modeling cloth", *IEEE Comp. Graph. & Appl.*, vol. 16, pp. 28-41, 1996.
- [10] M. Tarfaoui, J. Y. Drean and S. Aksebi, "Predicting the stress-strain behavior of woven fabrics using Finite Element Method", *Text. Res. J.*, vol. 71, no. 9, pp. 790-795, 2001.
- [11] G. A. V. Leaf and K. H. Kandil, "The initial load-extension behaviour of plain woven fabrics", *J. Text. Inst.*, vol. 71, pp. 1-7, 1980.
- [12] M. Tehrani Dehkordi, H. Nosraty and M. M. Shokrieh, "Prediction of tensile behaviour of hybrid-woven fabrics at initial extension", In: *Proceedings of the ATC11 conference*, South Korea; pp. 1066-1072, 2011.
- [13] J. W. S. Hearl and W. J. Shanahan, "An energy method for calculation in fabric mechanics part2: Examples of application of the method to woven fabrics", *J. Text. Inst.*, vol. 69, no. 4, pp. 92-100, 1978.
- [14] S. de Jone and R. Postle, "A physically-based particle model of woven cloth", *J. Text. Inst.*, vol. 15, pp. 376, 1977.
- [15] S. Jong and R. Postle, "A general energy analysis of fabric mechanics using optimal control theory", *Text. Res. J.*, vol. 48, no. 3, pp. 127-135, 1978.
- [16] S. de Jone and R. Postle, "An energy analysis of woven-fabric mechanics by means of optimal-control theory, Part II: pure-bending properties", *J. Text. Inst.*, vol. 68, pp. 362-369, 1977.
- [17] N. Khadamalhosseini, M. Nasr-Isfahani, M. Latifi and S. Shaikhzadeh-Najar, "Modeling of impact damage of sewing machine needle on woven fabric by finite element method", *J. Text. & Polym.*, vol. 1, no. 1, pp. 19-23, 2013.
- [18] J. Hu, *Structure and mechanics of woven fabrics*, Woodhead publishing in textiles, Cambridge: 2004.
- [19] Y. Shen, J. Meir, Y. Cao and S. Adanur, "Finite element analysis of monofilament woven fabrics under uniaxial tension", *J. Text. Inst.*, 2014.
- [20] Y. Hou, L. Jiang, B. Sun and B. Gu, "Strain rate effects of tensile behaviors of 3-D orthogonal woven fabric: Experimental and finite element analyses", *Text. Res. J.*, vol. 83, pp. 337-354, 2013.
- [21] P. Wang, Q. Ma, B. Sun, H. Hu, and B. Gu, "Finite element modeling of woven fabric tearing damage", *Text. Res. J.*, vol. 81, pp. 1273-1286, 2011.
- [22] Y. Jin Jeong and T. Jin Kang, "Analysis of compressional deformation of woven fabric using finite element method", *J. Text. Inst.*, vol. 92, pp. 1-15, 2001.

- [23] S. Dridi, A. Dogui and P. Boisse, "Finite element analysis of bias extension test using an orthotropic hyperelastic continuum model for woven fabric", *J. Text. Inst.*, vol. 102, pp. 781-789, 2011.
- [24] J. J. Lin, "Applying GM to predicting elastic property and FEM to analyzing tensile damage behavior for woven fabric" *J. Text. Inst.*, vol. 105, pp. 1029-1041, 2014.
- [25] R. Zouari, S. B. Amar and A. Dogui, "Experimental and numerical analyses of fabric off-axes tensile test", *J. Text. Inst.*, vol. 101, pp. 58-68, 2010.
- [26] T. J. Kang and W. R. Yu, "Drape simulation of woven fabric by using the finite-element method", *J. Text. Inst.*, vol. 86, pp. 635-648, 1995.
- [27] H. Hedfi, A. Ghith and H. Salah, "Study of dynamic drape behaviour of fabric using FEM, part I: model formulation and numerical investigations", *Inter. J. Eng. Sci. & Tech.*, vol. 3, pp. 6554-6563, 2011.
- [28] C. Mingxiang, S. Qingping and Y. Ming-fai "Simulation of fabric drape using a thin plate element with finite rotation", *Chinese J. Mech. Press*, vol. 14, pp. 239-245, 1998.
- [29] Abaqus Standard User's Manual, Ver.6.4.
- [30] J. W. S. Hearl, P. Grosberg, and S. Backer, *Structural mechanics of fibers, yarn and fabrics*, Willey-Interscience, Newyork: 1969.
- [31] S. Kawabata, N. Masako and H. Kawai, "The finite deformation theory of plain weave fabrics. Part2: the uniaxial deformation theory", *J. Text. Inst.*, vol. 64, no. 21, pp. 47-61, 1973.
- [32] M.J. Wilson, "Finite element analysis of glass fibre reinforced thermoplastic composites for structural automotive components", *Ph.D dissertation*, School of Mechanical, Materials, Manufacturing Engineering and Management, University of Nottingham, England, 2003.